Assessment of the Huygens' Box Method With Different Sources Near Obstacles

Sørensen, M.; Bonev, I. B.; Franek, O.; Pedersen, G. F.

Published in:
IEEE Transactions on Electromagnetic Compatibility

DOI (link to publication from Publisher):
10.1109/TEMC.2019.2908354

Publication date:
2020

Document Version
Accepted author manuscript, peer reviewed version

Assessment of the Huygens' Box Method With Different Sources Near Obstacles

Morten Sørensen, *Member, IEEE*, Ivan Bonev Bonev, Ondřej Franek, *Member, IEEE*, and Gert Frølund Pedersen, *Member, IEEE*

***Abstract*—The Huygens' box (HB) method allows an arbitrary printed circuit board (PCB) in a simulation to be replaced with a set of current sources on a closed surface. A numerical study of the method is performed with different noise sources, represented by its HB, in combination with different obstacles. The chosen combinations mimic radiation features of real PCBs and product environments. This study shows that if the ground plane and substrate are included in the HB, the accuracy of the HB method generally is good. However, if the coupling between the PCB and the obstacle is strong, the method fails at a few resonance frequencies. In the search for the methods general limits, it is shown that the method cannot predict the maximum radiated emission of power plane resonances without including the vias in the HB.**

***Index Terms*—Electromagnetic simulations, Huygen's box method, near-field scan, surface equivalence principle.**

I. Introduction

PRECOMPLIANCE test at printed circuit board (PCB) level makes it possible to estimate compliance early in a project. Several methods have been investigated over the years and a few standards for handling electromagnetic compatibility (EMC) at integrated circuit (IC) and PCB level have been written, e.g., IEC 61967 [1].

As clock frequencies increase, ICs, microstrips, and power-ground plane resonances increasingly radiate by themselves instead of being the source for common mode radiation by attached cables. With the right software installed on the PCB, one can measure the radiated emission from the PCB with power supply cable alone in a semi anechoic chamber (SAC) and get an estimate of the radiated emission from the final product caused by this PCB. However, enclosures and obstacles near the PCB can change the radiated emission significantly and, hence, methods for predicting radiation emission from PCBs, when it is mounted in a product, are needed.

Manuscript received October 5, 2018; revised February 5, 2019; accepted March 4, 2019. This work was supported by the Danish Agency for Science, Technology and Innovation. *(Corresponding author: Morten Sørensen.)*

M. Sørensen is with the EMC Laboratory, Missouri University of Science and Technology, Rolla, MO 65401 USA (e-mail: sorensenmo@mst.edu).

I. B. Bonev, O. Franek, and G. F. Pedersen are with the Antennas, Propagation, and Millimeter-Wave Systems Section, Department of Electronic Systems, Aalborg University, 9220 Aalborg, Denmark (e-mail: ibonev@mail.bg; of@es.aau.dk; gfp@es.aau.dk).

Color versions of one or more of the figures in this paper are available online at http://ieeexplore.ieee.org.

Digital Object Identifier 10.1109/TEMC.2019.2908354

A very ambitious idea is to measure the tangential component of the PCB's near field (E and H) and use the measured near fields as a source for simulation of the far field from the PCB mounted in the final product.

The scientific world has not yet agreed on a method and there are two different dominating approaches to the far-field prediction. One approach uses the near field as a basis for sources by help of an equivalent set of electric and/or magnetic dipoles [2]–[6] or ground current [7], whereas another approach uses tangential near fields on a surface entirely enclosing the module [8]–[13]. These fields that are distributed on the closed surface, named Huygens' box (HB), act as sources generating the same fields as the original sources on the PCB outside of this surface. The latter method is the basis of this paper and is often named the Huygens' box method.

Both methods are inaccurate when the PCB is measured in "free space" and afterward placed inside an enclosure or near an obstacle which interact with the source, (i.e., scattering and rescattering between source and enclosure/obstacle.) The limitation of the HB method follows directly from the theory, namely that a correct prediction of the field outside the HB requires that the near field is measured in the exact same environment as the environment used in the simulation of the far field outside the box.

In real products, PCBs will be mounted on a chassis, be inside an enclosure, and/or near cables, etc. In order to have the full benefits from the combination of near-field measurements and numerical methods, the simulations must take the scattering/rescattering into account. Studies of how to include this interaction are scarce. For the equivalent dipole method, the method can be extended to a dipole-dielectric conducting plane model to account for the interactions between the PCB and the enclosure by including the basic physical features of the PCB [2], [14].

A similar method can be used for the HB method. In previous works [15]–[18], a simple microstrip PCB was placed near a ground plane, a wire, and in two different enclosures. The microstrip PCB was replaced with its HB, and the maximum radiated emission from the microstrip and obstacles/enclosure was compared with the corresponding maximum radiation from the HB and the obstacles/enclosures.

The HB replacement could cause a significant error in the far-field prediction. However, these errors were below 2 dB if ground plane and dielectric of the PCB were included in the HB—except for a few resonance frequencies with very high Q factors. It was

also shown that if the PCB is grounded in the product, the near-field scan must also be carried out with grounding, otherwise the error could become significant.

In the above-mentioned works, the HB method was investigated only with one very simple PCB in simple environments. The method's relative success could be a possible coincidence. It was concluded that further studies were needed in order to make a trustworthy conclusion. The study presented in this paper elaborates on the above-mentioned HB studies [15]–[18]. With the purpose to substantiate the conclusions from the above-mentioned simple test cases, the method was tested with several, more complex, combinations of PCBs and environments mimicking typical radiation from PCBs in product. The models in previous work have predicted maximum far field with less than 2 dB error, except for very narrow banded strong resonances; therefore, focus in this study was to search for the method's general limitations.

This study is based solely on simulations instead of measurements with the purpose to isolate the observed inaccuracies to the HB method itself.

In Section II, the HB method is introduced and it is proved that including the full model inside the HB restores the fields outside in the presence of obstacles. The objectives of the simulations and different simulation scenarios are given in Section III. The results are presented and discussed in Section IV. Section V reviews the method based on the present study and previous studies, and draws the conclusions.

II. Huygens' Box Method

The ambitious idea is to characterize PCBs as HBs, (i.e., measure the tangential electric and magnetic near fields on a box enclosing the module.) In the following, the HB method simply describes a simulation, where the radiation from a PCB is represented by the tangential fields on a box surrounding the PCB. For a single PCB in open boundaries, the maximum radiated emission can be predicted based on near field to far field transformation of the HB. However, placing a module close to obstacles can change the radiated emission more than 20 dB, so the simple near-field far-field method does not work as a pre-compliance test when the EMC architecture of the product is included. Hence, the idea is to use a PCB's HB as a source for simulations.

A. With Homogeneous Medium

If the medium outside the HB is unchanged from the near-field scanning to the equivalent problem, it follows from Love's equivalent principle that the far field can be calculated from the HB. The principle states that a radiating source represented by electric and magnetic current densities $\vec{J}_1$ and $\vec{M}_1$, as shown in Fig. 1, is equivalent with electric and magnetic surface currents on a closed surface enclosing the original source [19]. These currents are related to the original fields $\vec{E}$ and $\vec{H}$ on the surface by

$$\vec{J}_s = \hat{n} \times \vec{H}_2|_S, \quad \vec{M}_S = -\hat{n} \times \vec{E}_2|_S \tag{1}$$

where $\hat{n}$ denotes the normal vector oriented outward the surface.

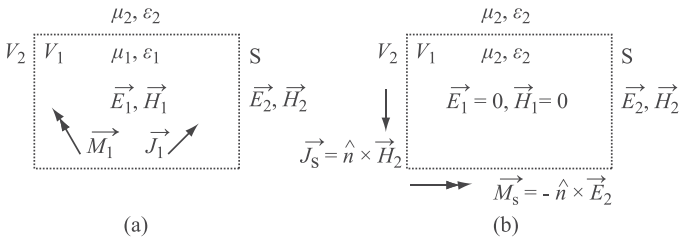

Fig. 1. Love's formulation of the surface equivalence problem. (a) Original problem. (b) Equivalent problem with surface currents—field inside is zero.

In Fig. 1, the enclosed surface is a box and denoted by Huygens' box, but the theory does not require a specific shape. The equivalent problem yields the same field outside the surface as the original problem. The fields inside the Huygens' box are zero [20].

B. Nearby Obstacles

In real cases, the medium outside the HB will change from the near-field scanning to the equivalent problem. The near-field scanning will be carried out in semi free space conditions after which the PCB is placed in a product where there will be obstacles nearby. It follows from an inside-out formulation of the traditionally formulated induction theorem [19] that if the full model is included inside the HB, the equivalent problem restores the original fields.

Let us assume a medium with constitutive parameters ϵ_1(sp), μ_1(sp), containing sources represented by electric and magnetic current densities $\vec{J}_1$ and $\vec{M}_1$, as shown in Fig 2(a), where "sp" indicates that the medium's parameters are a function of the space. These sources radiate the fields $\vec{E}_1$ and $\vec{H}_1$ everywhere. Now, let us assume that obstacles are placed outside the volume *V* whereby the medium outside *V* changes. The constitutive parameters of the medium are now ϵ_2, μ_2, as shown in Fig 2(b).

This obstacle perturbs the original field and the total field inside V_1 is now a superposition of the original field without obstacle and the scattered field from the obstacles

$$\vec{E} = \vec{E}_1 + \vec{E}_s \quad \vec{H} = \vec{H}_1 + \vec{H}_s \tag{2}$$

where $\vec{E}$ and $\vec{H}$ are the total field with the obstacle present, $\vec{E}_1$ and $\vec{H}_1$ are the original field without the obstacle, and $\vec{E}_s$ and $\vec{H}_s$ are the scattered fields due to the obstacle.

The transmitted field outside *V* is denoted by $\vec{E}_t$ and $\vec{H}_t$ and is the field of interest for the Huygens' box investigation. It can be calculated by help of an equivalent problem defined in Fig 2(c), which allows us to determine $\vec{E}_s$ and $\vec{H}_s$ inside *V* and $\vec{E}_t$ and $\vec{H}_t$ outside *V*. In Fig 2(c), the fields inside *V* are $\vec{E}_s$ and $\vec{H}_s$ and outside the fields are $\vec{E}_t$ and $\vec{H}_t$. In order to radiate such fields and satisfy tangential boundary conditions, it is necessary to introduce equivalent current densities $\vec{J}_i$ and $\vec{M}_i$

$$\vec{J}_i = \hat{n} \times (\vec{H}_\mathrm{s} - \vec{H}_\mathrm{t})$$
$$\vec{M}_i = -\hat{n} \times (\vec{E}_\mathrm{s} - \vec{E}_\mathrm{t}) \tag{3}$$

where $\hat{n}$ denotes the normal vector oriented inside *V*.

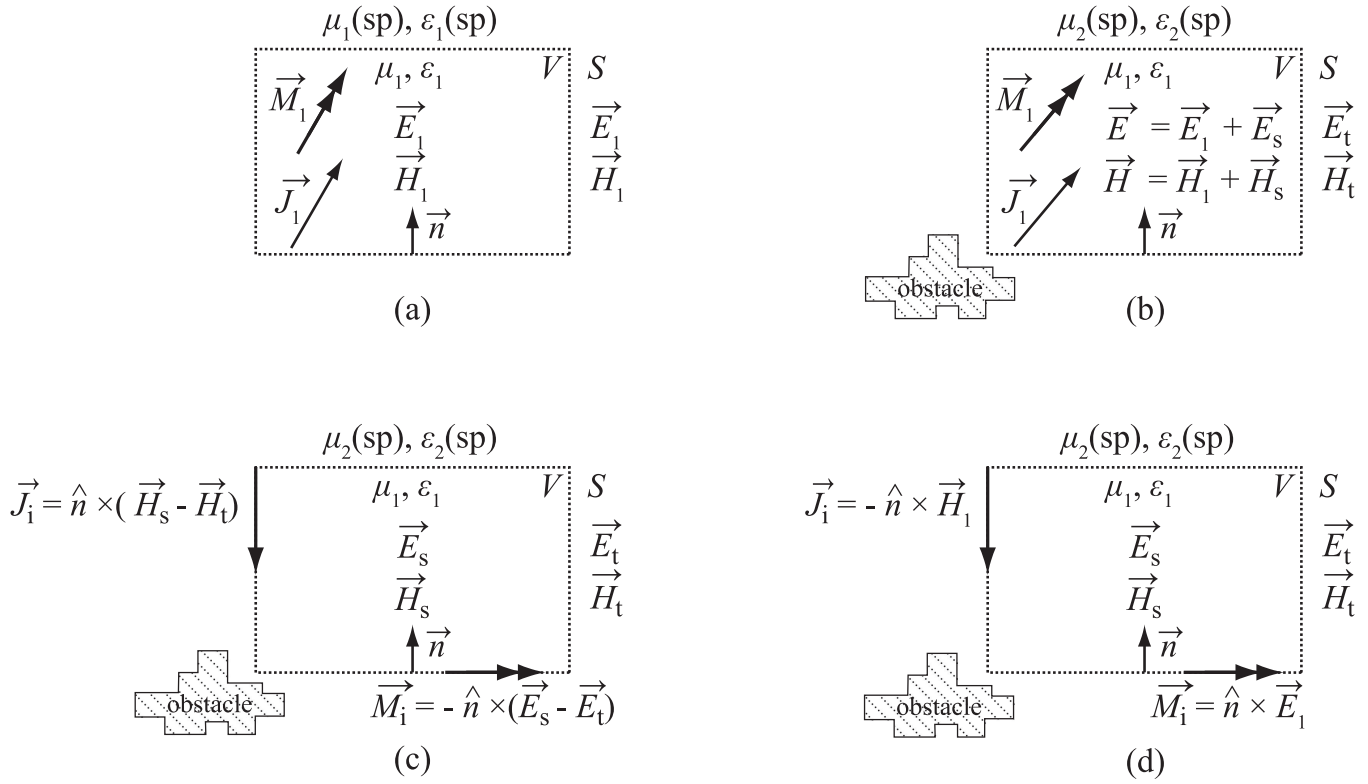

Fig. 2. Geometry for the inside out version of the induction theorem. (a) Sources in a homogeneous medium. (b) Homogeneous medium outside is replaced with an obstacle. (c) Equivalent problem. (d) Reduced equivalent problem.

The tangential components of the fields must be continuous across boundaries. Hence, Fig 2(b) implies that

$$\vec{E}_1|_{\tan} + \vec{E}_s|_{\tan} = \vec{E}_t|_{\tan}$$
$$\vec{H}_1|_{\tan} + \vec{H}_s|_{\tan} = \vec{H}_t|_{\tan}. \quad (4)$$

If (4) is rewritten and substituted into (2), the equivalent currents in Fig 2(c) can be written as

$$\vec{J}_i = -\hat{n} \times (\vec{H}_1)$$
$$\vec{M}_i = \hat{n} \times (\vec{E}_1). \quad (5)$$

With the new expression for the equivalent currents, the problem in Fig 2(c) can now be reduced to the equivalent in Fig. 2(d). Fig. 2(b)–(d) are all equivalent and, hence, the field outside the HB is the same in all problems. The equivalent currents in Fig. 2(d) are dependent purely on the original fields $\vec{E}_1$ and $\vec{H}_1$ without the obstacle as in Fig. 2(a), yet they perfectly recreate the fields around the obstacle as in Fig. 2(b). The condition is, however, that the original medium with constitutive parameters ϵ_1(sp), μ_1(sp) is included inside the HB. In practice, it means that it is possible to do a near-field scan in "free space" condition and then use the "free space" measured tangential field as a source for simulations of near obstacles as long as the scanned PCB is included in the HB. Of course, it is of no use if it is necessary to include all details in the HB, because then it would be easier to just do a full wave simulation of the PCB, but if it is possible to judge which elements of the PCB that are responsible for the scattering, one could approximate the field by including the most important parts of the PCB.

This section shows that the HB method reproduces the radiated emission without errors in two different cases.

1) The medium outside the HB is unchanged from the near-field measurement to the equivalent problem. This corresponds, for example, to a setup where the far field from a PCB alone is calculated from a near-field scan in "free space."
2) The medium outside the HB changes from the near-field measurement to the equivalent problem, but the original medium inside the HB is included in the equivalent problem. This corresponds to a setup where a near-field scan is performed in "free space" and the measured HB is used as a source for simulation where the full model of the DUT is placed inside the HB.

In practice, this will typically be something between cases 1 and 2. The near-field scan will be carried out in "free space," but it is not possible in practice to include the full physical model of the DUT in the simulation. This will introduce an error depending on source and obstacles. The error cannot be generalized, but simulations of different combinations of source and obstacles can give a figure of the introduced error.

III. Simulations Setup

The purpose of this study was to investigate the HB method near obstacles in further details, and especially search for its

general limitations. Hence, a number of PCB structures were placed in different environments and tested by simulations.

A. Numerical Details

All simulations were carried out with an in-house numerical code implementing the finite-difference time-domain (FDTD) method [21].

The implementation has uniform spatial discretization so the number of mesh cell is proportional with (1/cell size)^3. In addition, the time step is proportional with cell size. Therefore, a halving of the mesh size will increase the duration of the simulation by 16 times. The importance of the discretization was discussed in [17] and it was shown that mesh size could slightly change the "bad" frequencies, but not the overall amplitude differences between the reference and the HB simulations. Based on these results, we chose 2-mm mesh cells and perfectly matched layers as the absorbing boundary condition. 2 mm correspond to $\frac{1}{75}$ wavelength in FR4 at 1 GHz.

The time step for the cell size of 2 mm was $\Delta t = 3.8483 \cdot 10^{-12}$ s. The majority of the simulations have number of time steps between 30 000 and 100 000, but some of the resonance frequencies required up to several million time steps before the total energy in the system was reduced 30 dB from maximum and the simulation was terminated.

The HB implementation in to the code, i.e., using near-field sources, does not yet allow wide band excitation of near-field sources. Hence, the HB method was evaluated at frequencies from 20 MHz to 1 GHz, with a 20-MHz step, and, in addition, some frequencies were added at which resonances occur. The simulation input power was 0 dBm.

B. Workflow

The workflow of the simulations is illustrated in Fig. 3.

1) A full model of the PCB was simulated in free space and the tangential components of the E- and H-fields on an HB 10 mm around the structure was extracted, as shown in Fig. 3(a). 10 mm correspond to a typical scanning height.
2) The far field from the radiating structure placed in a reflective environment was simulated as reference. This is illustrated in Fig. 3(b).
3) The radiating structure was replaced by the equivalent sources from 1) with an empty HB as shown in Fig. 3(c).
4) Parts of the radiating structure (e.g., ground plane and substrate) were included in the HB in order to take scattering into account, as shown in Fig. 3(d).
5) With the purpose to validate the simulation, the full radiating structure was included in the Huygens' box, as shown in Fig. 3(e). The full structure was passive, (i.e., the structure was not excited, but the 50 Ω source impedance was still present.)

C. Sources

Three categories of PCB sources were used in the simulations. The sources mimic typical unwanted radiated emission from PCBs, namely radiation from a microstrip, an IC, and power planes.

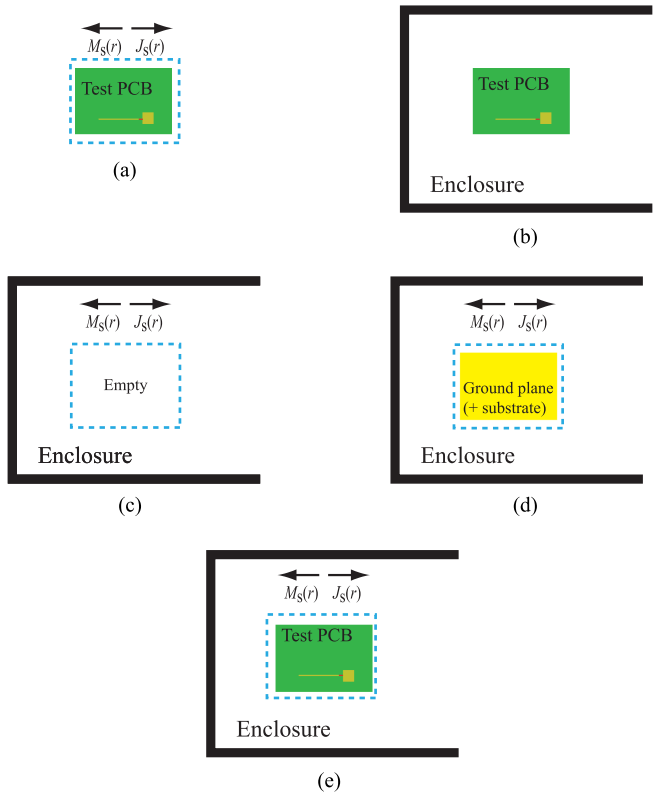

Fig. 3. Simulation workflow. (a) PCB in free space. (b) PCB in enclosure. (c) Empty HB in enclosure. (d) HB with main features in enclosure. (e) HB with full model in enclosure.

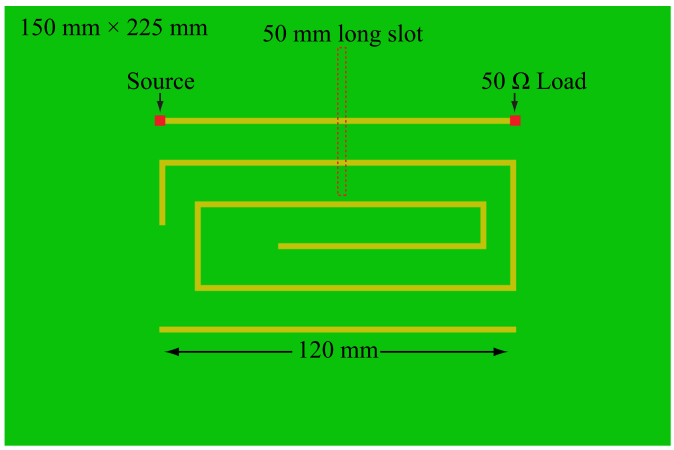

Fig. 4. Simple microstrip above a 150 × 225 mm ground plane. Both a version with unbroken ground plane, and a version with a slot in the ground plane were used in the analysis.

1) 50 Ω Microstrip—Source 1: A simple 150 mm × 225 mm two-layer PCB with three traces on the top was modeled, as shown in Fig. 4. The substrate was a 2-mm thick lossy FR4 layer with relative permittivity 4.35 and conductivity 10^{-3} S/m. Only the upper trace was excited and terminated. The lower trace and spiral formed trace were floating in order to make possible resonances. The active trace was 120 mm long and 2 mm wide and both source and load impedances were 50 Ω. A version with a 50-mm long orthogonal slot in the ground plane below the trace

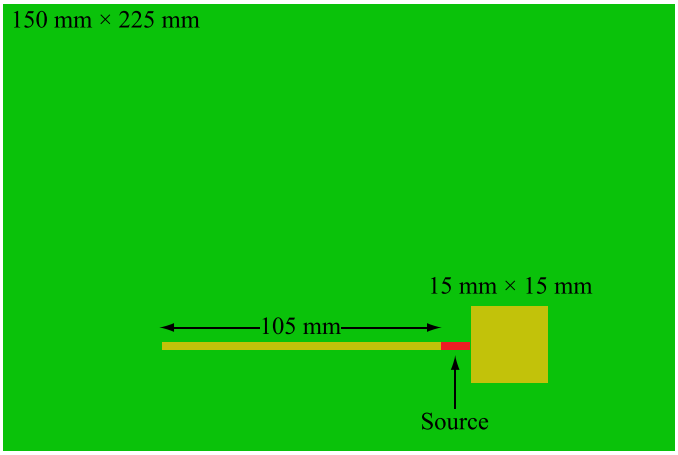

Fig. 5. Microstrip connected to an IC on a PCB.

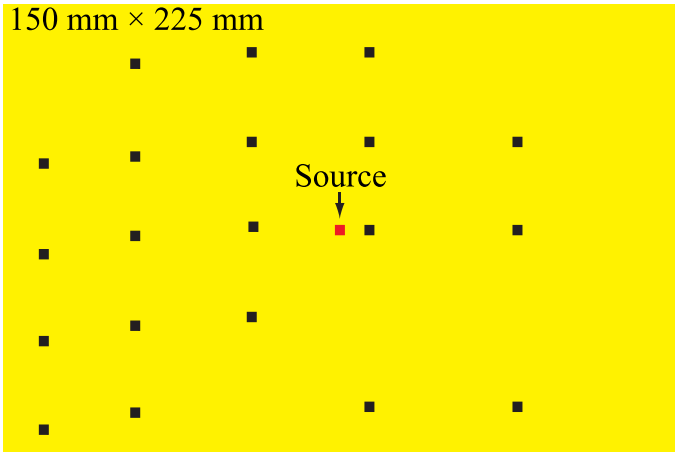

Fig. 6. Two ground planes with 19 randomly distributed vias excited with a port between them.

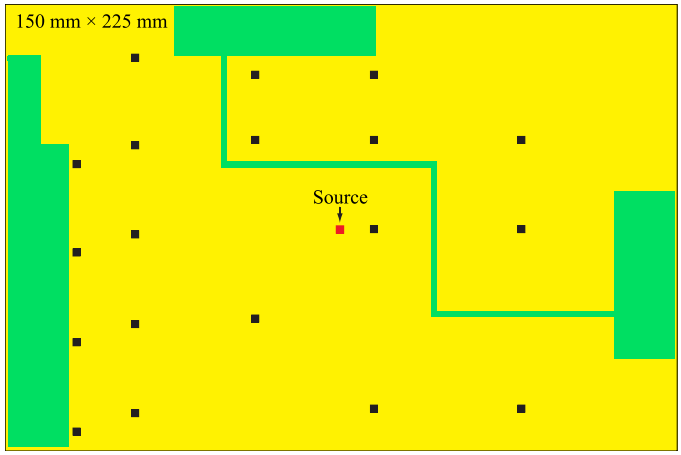

Fig. 7. Full ground plane with two separated ground fill and 19 vias.

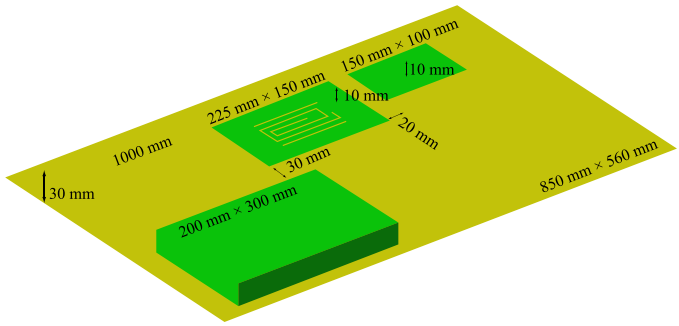

Fig. 8. Microstrip PCB in a TV set environment with several scatters near the radiating source.

was also used. The slot changes the near-field significant and radiated emission is increased several dBs because of the slot.

2) IC/Heat Sink Radiation—Source 2: The three traces were replaced by a microstrip connected to a 15 × 15 mm flat metal plate mimicking a radiating IC. The PCB is shown in Fig. 5.

3) Power-Ground Plane Resonances—Source 3: Two 150 × 225 mm ground planes were excited with a port between the planes mimicking radiating plane resonances, as shown in Fig. 6. A total of 19 vias, connecting the planes, were distributed over the board. In one version, the board was excited in the center and in another version, the board was excited in the corner.

A more complicated version of the above-mentioned PCB was also used as a source. The full-size top ground plane was replaced with a more typical ground fill consisting of two irregular ground fill separated from each other, as shown in Fig. 7. The model was excited with a 50 Ω port between the large left ground fill and the bottom full ground plane.

D. Obstacles

Two different environments were used in the investigation. A large ground plane with a wire, a metal box, and a ground plane near the source, mimicking a TV set was used for further investigation of the method. A narrow enclosure serving as worst case was used in the search for the limits of the method.

1) Ground Plane, Wire, and Metal Box—Environment 1: The method was tested in an environment mimicking a TV set. The source PCB was placed floating 2 cm above a 85 cm × 56 cm large ground plane. A 1-m long wire was placed 1 cm above the radiating PCB (mimicking poor EMC design that sometimes is unavoidable). Another 20 cm × 30 cm metal structure was placed 3 cm away from the radiating PCB, and a 10 × 15 cm metal plate was placed 2 cm away from the radiating PCB. Two different cabling routes were tested. The two routes were a cable in an L-shape in contact with the ground plane, as shown in Fig. 8, and a long straight floating wire. The overall purpose with this structure was to test the HB method in an environment with several scatterers near the radiating source.

2) Narrow Enclosure—Environment 2: In the search for the general limit of the method, the radiating PCBs were placed in the center of a narrow enclosure with the dimension 450 mm × 300 mm × 40 mm and open in one end, as shown in Fig. 9. With a height of only 40 mm, the enclosure was placed in the reactive near field of the PCB and the HB. The radiated field will be scattered and rescattered multiple times.

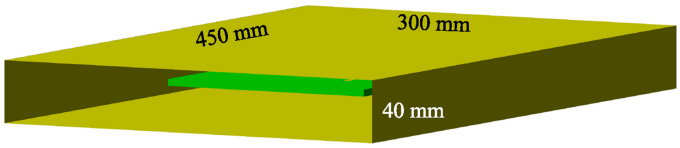

Fig. 9. Radiating PCBs were placed in a narrow enclosure open in one end.

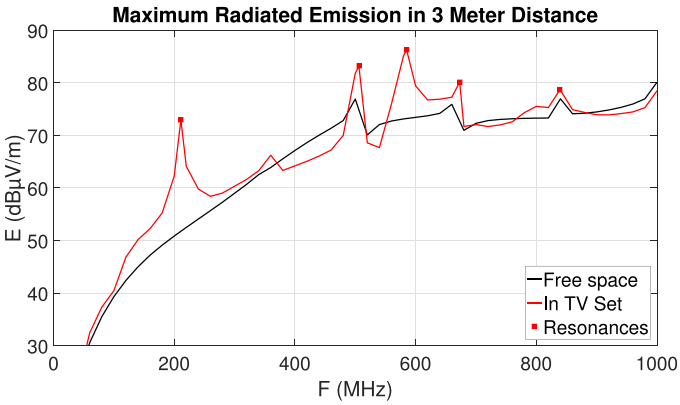

Fig. 10. Maximum radiated emission in 3-m distance from the microstrip PCB in free space versus in the TV set environment. Resonances are denoted by squares.

IV. Results and Discussion

The maximum field is the focus in an EMC-radiated emission measurement. Hence, in all scenarios, the errors introduced by the HB method were evaluated as the difference in the far field between the HB simulations and the reference

$$\text{Far-field error} = 20 \cdot \log_{10} \frac{\max(E_{\text{Huygens'}})}{\max(E_{\text{reference}})} \tag{6}$$

where, $\max(E_{\text{Huygens'}})$ is the maximum far E-field of the Huygens' Box model and $\max(E_{\text{reference}})$ is the maximum far E-field of the reference case. The maximum is taken across both theta and phi components — equivalent to the difference in two far-field measurements according to CISPR 35. However, the field is evaluated on the whole sphere, and no conductive floor is included in the evaluation. It is somewhat subjective what is acceptable for far-field errors caused by the HB method. If the errors are below 2 dB, it is still significantly smaller than the common 6-dB measurement uncertainty in the EMC society.

With the purpose to obtain a reliable conclusion, the method was tested in different cases. However, due to the limited number of pages, only some representative or illustrative examples are presented in details and the rest of the results are only briefly summarized.

A. Microstrip PCB in TV Set Environment

The PCB with three microstrips and an unbroken ground plane (source 1) was placed in the TV set (environment 1), as shown in Fig. 8. Fig. 10 shows the radiated emission in 3-m distance for the PCB in free space versus the PCB in the TV set environment with the L-shaped cable 20 mm above the PCB. As one would expect, the radiated emission increases up to 22 dB when the cable is placed above the PCB.

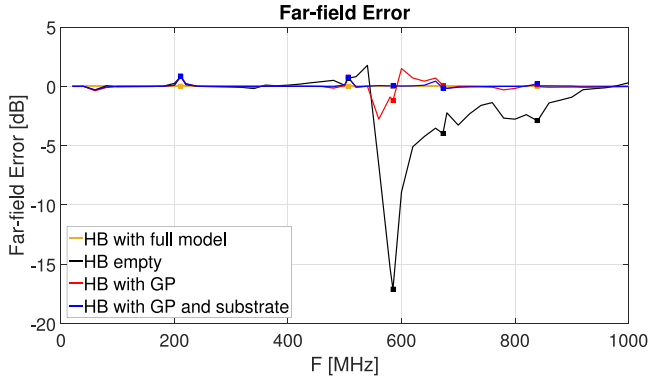

Fig. 11. Far-field errors for the microstrip PCB in TV set environment. Resonances are denoted by squares.

The setup mimics a situation where wrong EMC design with a cable above a PCB is unavoidable. The question is whether it is possible from near-field scan and simulation to predict radiated emission from a specific cabling and several scatterers nearby the source.

The far-field errors for the L-shaped grounded cable are shown in Fig. 11. In Section II-B, it was proved that including the full model inside the HB restores the fields outside the HB in the presence of obstacles. The far-field errors for HB full model were 0 dB as expected, which served as a control of the HB method implementation in the FDTD code. When the HB was empty, the far-field errors became considerable, e.g., at 581 MHz where an empty HB underestimated the radiated emission by 17 dB. Ground plane and substrate are a part of the resonating system at 581 MHz. Without these features, the HB method does not recreate the resonator. If the ground plane was included in the HB, the far-field errors were reduced to a maximum of 2.8 dB. If the lossy substrate was included also, the far-field errors were reduced to less than 1 dB — even at resonance frequencies.

The results for the floating wire were very similar. Maximum absolute far-field error with ground plane included was 2.3 dB, and when the substrate was also included, the absolute far-field errors were reduced to less than 0.5 dB — even at resonance frequencies.

B. Microstrip and IC/Heatsink PCB in Narrow Box

The microstrip PCB with a slot in the ground plane below the trace (source 1), as well as the IC/heat sink PCB (source 2) were placed in the narrow enclosure (environment 2). When the sources were placed in the narrow box, the maximum radiated emission decreased up to 20 dB at lower frequencies. From 400 MHz and up, the radiated emission both decreased and increased because of the box.

The far-field errors introduced by the HB method for the microstrip PCB with a slot in ground plane are shown in Fig. 12. A surprising fact is that the empty HB and the HB with only a ground plane caused almost the same far-field errors,

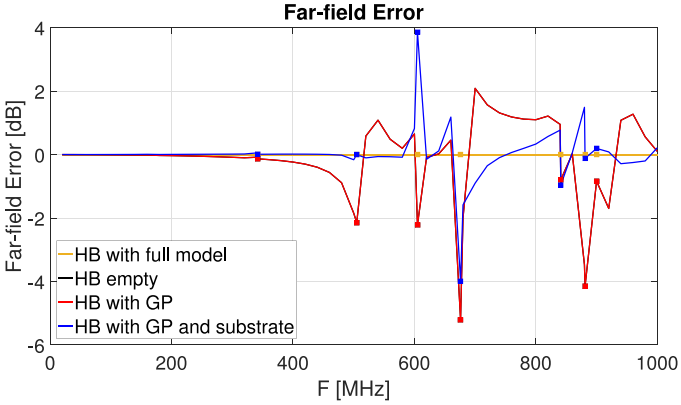

Fig. 12. Far-field errors for the microstrip PCB with slot in the ground plane inside the narrow box. Resonances are denoted with a square.

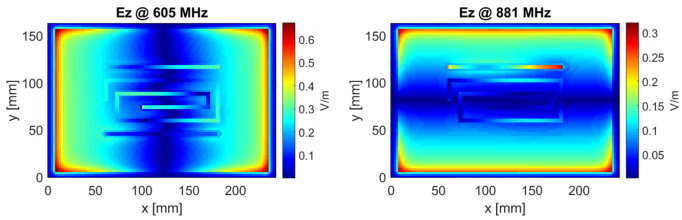

Fig. 13. Orthogonal E-field right above the trace layer. Left: TE10 mode at 605 MHz. Right: TE01 mode at 881 MHz.

(i.e., the black and red curves coincide in Fig. 12). One explanation could be that only TExx modes are excited in the enclosure, which have the E-field orthogonal to the ground plane, and so adding the ground plane does not affect the fields. When the substrate is added, the speed of propagation changes (in all directions), and the field distribution is changed, including the resonance frequency. Modes 01 and 10 are shown in Fig. 13.

The result is similar to the microstrip in a TV set environment. An empty HB introduces up to 6 dB error, however, if the ground plane and substrate are included in the HB, the errors are, in general, reduced to less than 1 dB. In contrast to the TV set, the far-field errors do not drop to an acceptable level at the resonance frequencies even with the ground plane and the substrate included in the HB. At 605 and 676 MHz, the far-field errors are 4 and -4 dB, respectively.

The far-field errors for the IC/heatsink PCB in the narrow box were very similar. In general, the far-field error introduced by the HB method was below 1 dB if ground plane and substrate were included in the HB. However, at the resonance frequency 603 MHz, the far-field error again was -4 dB.

The only features making the difference from the full model, with 0 dB far-field error, are the traces and the 50-Ω loads for the microstrip PCB, and the trace and IC/heatsink for the other PCB. At a glance, this is quite surprising. However, the observed strong resonances between the PCB and the box have a very high Q factor and correspondingly narrow bandwidth. Fig. 13 shows that the orthogonal E-field concentrates above the traces and, hence, the floating traces are a part of the resonating system consisting of the microstrip PCB and the narrow box. This resonance is

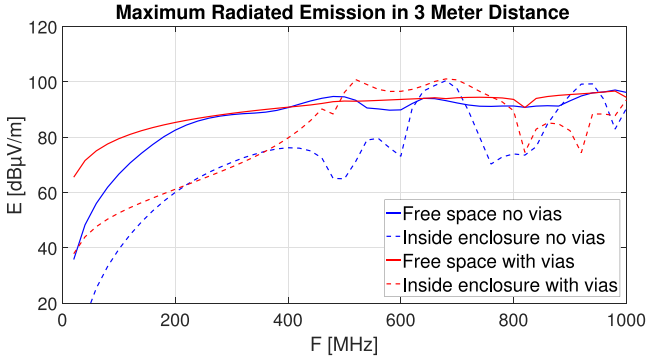

Fig. 14. Maximum radiated emission with and without vias and in free space and inside enclosure.

detuned without all features, (i.e., ground plane, substrate, and traces). For the TV set in contrast, the resonances are primarily caused by the wire that has a lower Q factor compared to the narrow box.

C. Ground Plane Resonances in Narrow Box

Until now, the HB method has only failed for a few narrow banded resonances caused by strong interaction between source and environment. In the search for the general limit of the method, the question arose of what happens if the important features of the PCB included in the HB are a part of the source for radiation. Hence, a PCB with two ground planes (source 3, Fig. 6) was simulated in free space and floating in the center of the narrow enclosure (environment 2, Fig. 9). The maximum radiated emission in 3-m distance for the ground plane excited in the center, with and without 19 vias, is shown in Fig. 14. The results are shown in order to illustrate that the vias change both the amplitude and resonance frequencies of the radiated emission from the PCB. When the via PCB was placed inside the narrow enclosure, the maximum radiated emission changed up to 30 dB compared to a free space simulation of the via PCB. This illustrates the potential usability of the method, because, if a free space radiated emission measurement of a PCB is used as precompliance test, it will deviate much from the radiation of the apparatus that the PCB will be mounted.

Above 400 MHz, the radiation from the PCBs (with and without vias) does not variate much in free space. However, when the boards are placed inside the enclosure, there is up to 30-dB difference between the PCB with and without vias indicating a complex resonance system depending of the vias. If these differences are caused by the different near fields (i.e., the different HBs), there is no problem for the HB method. On the other hand, if the differences are caused by strong coupling between the board and enclosure, this coupling will depend on the numbers and location of the vias. Hence, the vias will be a major feature that must be included in the HB simulation. This will require detailed knowledge about the PCB layout reducing the usability of the HB method.

The far-field errors for the via PCB with excitation in center are shown in Fig. 15. When the ground plane was included in the

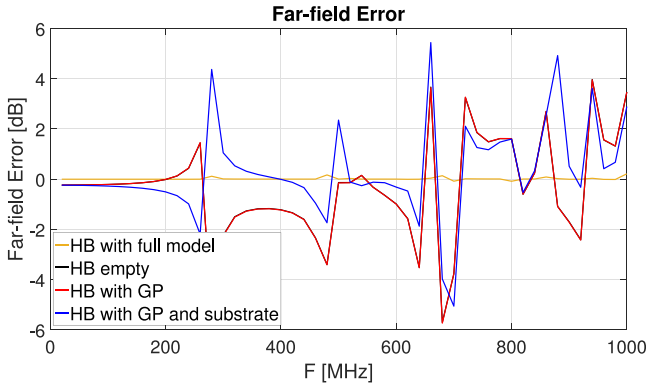

Fig. 15. Far-field error for the via PCB inside the narrow box.

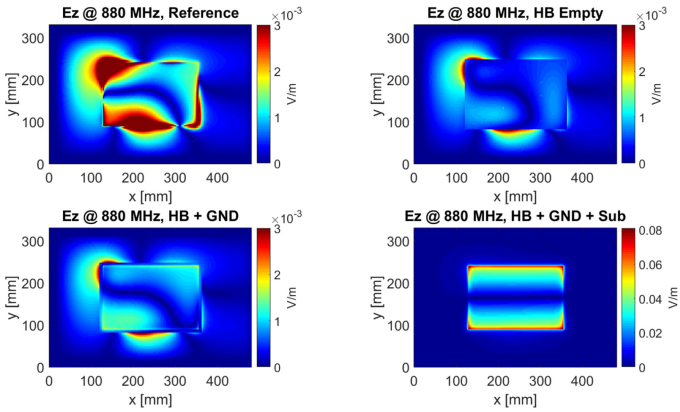

Fig. 16. Orthogonal E-field just above the via PCB.

HB, it was without the vias. Again, the empty HB and the HB with only ground planes (no vias) caused almost the same far-field errors. Also the far-field errors changed when the substrate was included. The far-field errors were between ± 6 dB over the whole frequency span not limited to a few resonance frequencies. The far-field errors of the HB, with full model, is included in Fig. 15 in order to prove that the differences are positively caused by the different features included in the HB and not numerical errors.

Fig. 16 shows the orthogonal E-field just above the via PCB inside the narrow enclosure at 880 MHz. The near field of the full model (reference), empty HB, and HB + GND looks similar with almost same amplitude. This is in agreement with the fact that the empty HB and the HB with GND estimate the maximum radiated emission within 1 dB. However, if the substrate is included as well, the TE01 mode is excited and the maximum radiated emission is overestimated with 5 dB. This is the same TE01 mode that was excited for the microstrip board, as shown in Fig. 13. This mode exist only with the substrate present and, hence, the large difference with and without substrate. This mode does not exist when the two ground planes are connected with a number of vias.

If the board was excited in the corner instead of the center, the far-field errors were very similar. The errors have similar amplitude (±6 dB) but is located at different frequencies.

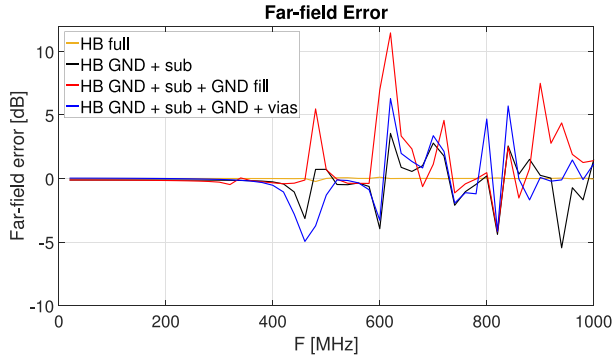

Fig. 17. Far-field error for the ground fill PCB inside the narrow box.

D. Ground Fill Board in Narrow Box

The results in the previous section, indicated that vias can be a major feature for the HB method and hence required to be include in the HB for reliable results. Many two-layer PCBs have a ground plane and a top layer partly covered with ground fill. The ground fill board shown in Fig. 7 was placed floating in the center of the narrow enclosure.

The far-field errors for the HB filled with different features are shown in Fig. 17. It has already been shown that the substrate is important for the method, so it was included in all cases. The substrate was combined with the ground plane (GND + sub), ground plane, and ground fill (but no vias) (GND + sub + GND fill), and finally two full-size ground planes, (i.e., the top ground plane was full size and not the ground fill) with the vias (GND + sub + GND + vias). In all cases, the HB method introduces significant far-field errors from 400 MHz and up. Including everything except the vias is actually worst case, and shows that the vias are a major feature for the coupling between the narrow box and the PCB. If the vias are included with full ground plane instead of the ground fill, it also causes significant far-field errors, hence, the ground fill is also a major feature of the coupling.

V. Conclusion

When a PCB is placed in a product, the maximum radiated emission can change up to ±30 dB compared to a free space measurement. Hence, a free space measurement of the PCB does not serve as a precompliance test. If the PCB's near field on a closed surface is used as a source for simulation, it is, in many cases, possible to estimate the far field of the PCB near obstacles with high accuracy by a combination of near-field measurements and simulations.

Several combinations of sources and environments have been investigated in this paper and [17] and [18]. The different combinations and the far-field errors caused by the HB method are summarized in Table I.

The results indicate that generally the HB method can predict very large changes in far field caused by obstacles only with small errors (less than 1 dB) if the environment does not have strong resonances. The results also indicate that the far-field error will increase with the Q factor of the resonances. Resonances are

TABLE I
FAR-FIELD ERRORS INTRODUCED BY THE HB METHOD

Source	Environment	Far-field errors caused by the HB methode
Microstrip PCB, unbroken ground plane.	TV set	Less than 1 dB error with ground plane and substrate included – even at resonance frequencies
Microstrip PCB, unbroken ground plane.	Half open box (50 cm × 30 cm × 15 cm)	Less than 1 dB error with ground plane and substrate included – even at resonance frequencies [17]
Microstrip PCB, unbroken ground plane.	Narrow box (environment 2)	In general less than 2 dB error with ground plane and substrate included. However, at a few resonance frequencies there were up to 10 dB far-field error [18]
Microstrip PCB with a slot under the trace (the slot is the noise source)	Narrow box (enviroment 2)	In general less than 1 dB error with ground plane and substrate included. However, at a few resonance frequencies there were 4 dB error.
IC / heatsink PCB	Narrow box (environment 2)	In general less than 1 dB error with ground plane and substrate included. However, at one resonance frequencies the error was 4 dB.
Power plane resonance between two planes connected with 19 vias	Narrow box (enviroment 2)	Unacceptable far-field errors up to 6 dB with ground planes and substrate included. The errors were not restricted to a few resonance frequencies.
Two layer PCB with ground fill and 19 vias	Narrow box (enviroment 2)	No matter which parts that were included in the HB, the method caused unacceptable far-field errors up to 10 dB. The errors were not restricted to a few resonance frequencies.

often the problem when radiated emission test fail, and, hence, the accuracy of the method is limited with respect to resonance structures with high Q. However, this study has searched for the limitations of the method and a general conclusion cannot be made based on this finite set of setups. Despite the inaccuracies, the method is still useful with respect to predicting trends and point out possible problems that cannot be predicted by measuring the radiated emission from the PCB alone. To achieve best practice for accuracy, the engineer makes use of electromagnetic understanding, as well as understanding of which features of the PCB that are a part of possible resonances. The method finds a general limit when the far field are predicted from PCBs, with plane resonances, placed in a resonant environment. In that case, the unacceptable far-field errors are not restricted to a few resonance frequencies. This study has only investigated the numerical errors introduced by the HB method. On top of that, the method is off cause also sensitive to measurement uncertainty and errors.

ACKNOWLEDGMENT

The authors would like to thank the Danish e-Infrastructure Cooperation for the hybrid Linux cluster "Fyrkat" at Aalborg University, Denmark.

REFERENCES

[1] *Integrated Circuits Measurement of Electromagnetic Emissions, 150 kHz to 1 GHz*, IEC 61967, 1st ed., 2003.
[2] X. Tong, D. W. P. Thomas, A. Nothofer, P. Sewell, and C. Christopoulos, "Modeling electromagnetic emissions from printed circuit boards in closed environments using equivalent dipoles," *IEEE Trans. Electromagn. Compat.*, vol. 52, no. 2, pp. 462–470, May 2010.
[3] Y. Vives-Gilabert, C. Arcambal, A. Louis, F. de Daran, P. Eudeline, and B. Mazari, "Modeling magnetic radiations of electronic circuits using near-field scanning method," *IEEE Trans. Electromagn. Compat.*, vol. 49, no. 2, pp. 391–400, May 2007.
[4] M. Hernando, A. Fernandez, M. Arias, M. Rodriguez, Y. Alvarez, and F. Las-Heras, "EMI radiated noise measurement system using the source reconstruction technique," *IEEE Trans. Ind. Electron.*, vol. 55, no. 9, pp. 3258–3265, Sep. 2008.
[5] Z. Yu, J. A. Mix, S. Sajuyigbe, K. P. Slattery, and J. Fan, "An improved dipole-moment model based on near-field scanning for characterizing near-field coupling and far-field radiation from an IC," *IEEE Trans. Electromagn. Compat.*, vol. 55, no. 1, pp. 97–108, Feb. 2013.
[6] B. Wang, E. Liu, W. Zhao, and C. E. Png, "Reconstruction of equivalent emission sources for PCBs from near-field scanning using a differential evolution algorithm," *IEEE Trans. Electromagn. Compat.*, vol. 60, no. 6, pp. 1670–1677, Dec. 2018.
[7] Q. Huang *et al.*, "Mom-based ground current reconstruction in RFI application," *IEEE Trans. Electromagn. Compat.*, vol. 60, no. 4, pp. 1121–1128, Aug. 2018.
[8] J. Shi, M. Cracraft, J. Zhang, R. DuBroff, and K. Slattery, "Using near-field scanning to predict radiated fields," *Proc. Int. Symp. Electromagn. Compat.*, Aug. 2004, vol. 1, pp. 14–18.
[9] H. Weng, D. G. Beetner, and R. E. DuBroff, "Prediction of radiated emissions using near-field measurements," *IEEE Trans. Electromagn. Compat.*, vol. 53, no. 4, pp. 891–899, Nov. 2011.
[10] X. Gao, J. Fan, Y. Zhang, H. Kajbaf, and D. Pommerenke, "Far-field prediction using only magnetic near-field scanning for EMI test," *Electromagn. Compat., IEEE Trans.*, vol. 56, no. 6, pp. 1335–1343, Dec. 2014.
[11] L. Foged *et al.*, "Bringing numerical simulation and antenna measurements together," in *Proc. 8th Eur. Conf. Antennas Propag.*, Apr. 2014, pp. 3421–3425.
[12] M. Sørensen, O. Franek, and G. F. Pedersen, "Recent developments in using measured sources in computational EMC," in *Proc. 9th Eur. Conf. Antennas Propag.*, May 2015, pp. 1–5.
[13] L. Li *et al.*, "Radio-frequency interference estimation by reciprocity theorem with noise source characterized by Huygens's equivalent model," in *Proc. IEEE Int. Symp. Electromagn. Compat.*, Jul. 2016, pp. 358 363.
[14] X. Tong, D. W. P. Thomas, A. Nothofer, P. Sewell, and C. Christopoulos, "Reduction of sensitivity to measurement errors in the derivation of equivalent models of emission in numerical computation," in *Proc. IET 8th Int. Conf. Comput. Electromagn.*, Apr. 2011, pp. 1–2.
[15] O. Franek, M. Sorensen, H. Ebert, and G. Pedersen, "Influence of nearby obstacles on the feasibility of a Huygens' box as a field source," in *Proc. IEEE Int. Symp. Electromagn. Compat.*, Aug. 2012, pp. 600 604.
[16] O. Franek, M. Sorensen, H. Ebert, and G. Pedersen, "Near-field characterization of a printed circuit board in the presence of a finite-sized metallic ground plane," in *Proc. Prog. In Electromagn. Res. Symp.*, Mar. 2012, pp. 1146–1149.
[17] M. Sorensen, I. Bonev, O. Franek, G. Petersen, and H. Ebert, "How to handle a Huygens' box inside an enclosure," in *Proc. IEEE Int. Symp. Electromagn. Compat.*, Aug. 2013, pp. 802–807.
[18] O. Franek, M. Sørensen, I. B. Bonev, H. Ebert, and G. F. Pedersen, "Influence of resonances on the Huygens' box method," in *Proc. Int. Symp. Electromagn. Compat.*, Sep. 2013, pp. 381–384.
[19] C. A. Balanis, *Advanced Engineering Electromagnetics*. New York, NY, USA: Wiley, 1989.
[20] S. Rengarajan and Y. Rahmat-Samii, "The field equivalence principle: illustration of the establishment of the non-intuitive null fields," *IEEE Antennas Propag. Mag.*, vol. 42, no. 4, pp. 122–128, Aug. 2000.
[21] A. Taflove and S. C. Hagness, *Computational Electrodynamics: The Finite-Difference Time-Domain Method*, 3rd ed. Boston, MA, USA: Artech House, 2005.

Morten Sørensen (M'08) received the M.S. degree in physics from Aarhus University, Aarhus, Denmark, in 2005, and the Ph.D. degree in wireless communications from Aalborg University, Aalborg, Denmark, in 2018.

From 2006 to 2017, he was an Antenna and Electromagnetic Compatibility (EMC) specialist with Bang & Olufsen, Struer, Denmark, including three years (2011–2014) as a Researcher and Technical Project Manager in the innovation consortium, "EMC Design—First Time Right." In 2017, he joined the EMC Laboratory, Missouri University of Science and Technology, Rolla, MO, USA, where he is a Visiting Assistant Research Professor. Since 2018, he has been working part time with Amber Precision Instruments, San Jose, CA, USA. His current research interests include near-field scanning, emission source microscopy, electrostatic discharge, and system-level radiated emission.

Ivan Bonev Bonev received the B.Sc. and M.Sc. (Hons.) degrees in telecommunications and the M.Sc. degree in electrical engineering from the Technical University of Varna, Varna, Bulgaria, in 2002, 2004, and 2007, respectively, and the Ph.D. degree in wireless communications from Aalborg University, Aalborg, Denmark, in 2013.

He was a Visiting Researcher with Ecole Politechnique de l'Universite de Nantes, Nantes, France; Tampere University of Technology, Tampere, Finland; and Atlantic Cape Community College, Cape May Court House, NJ, USA. His research interests include antennas, theoretical aspects of antenna systems, antenna interactions with a human body, hearing aid compatibility of mobile phones, and specific absorption-rate problems.

Dr. Bonev was the recipient of the URSI Young Scientist Award in group B Waves and Fields for 2011.

Ondřej Franek (S'02–M'05) received the Ing. (M.Sc.E.E. Hons.) and Ph.D. degrees in electronics and communication technology from the Brno University of Technology, Brno, Czech Republic, in 2001 and 2006, respectively.

He is currently an Associate Research Professor with the Department of Electronic Systems, Aalborg University, Aalborg, Denmark, where he is a member of the Antennas, Propagation, and Millimeter-Wave Systems Section. His research interests include electromagnetic theory and computational electromagnetics with a focus on fast and efficient numerical methods, especially the finite-difference time-domain method. He has developed the in-house fully scalable parallel FDTD code that has been used in research at Aalborg University to solve electrically large problems related to antennas, radiowave propagation, and electromagnetic compatibility.

Dr. Franek was a recipient of the Seventh Annual Siemens Award for outstanding scientific publication.

Gert Frølund Pedersen (M'14) received the B.Sc. and E.E. (Hons.) degrees in electrical engineering from the College of Technology in Dublin, Dublin Institute of Technology, Dublin, U.K., in 1991, and the M.Sc.E.E. and Ph.D. degrees from Aalborg University, Aalborg, Denmark, in 1993 and 2003, respectively.

Since 1993, he has been with Aalborg University where he is currently a Full Professor heading the Antennas, Propagation and Millimeter-Wave Systems Lab with 25 researchers. He is also the Head of the Doctoral School on Wireless Communication with some 40 Ph.D. students enrolled. He has authored or coauthored more than 500 peer-reviewed papers, six books, 12 book chapters and holds more than 50 patents. His research interests include radio communication for mobile terminals, especially small antennas, diversity systems, propagation, and biological effects.